

Supporting Information

ACHIEVING HIGHLY EFFICIENT ANTISOLVENT- AND ANNEALING-FREE NIR PEROVSKITE LIGHT-EMITTING DIODES BY OPTIMIZING GRADIENT OF PREHEATING

Johan Iskandar, Chih-Chien Lee, Xiang Ren Deng, Shun-Wei Liu, and Sajal Biring

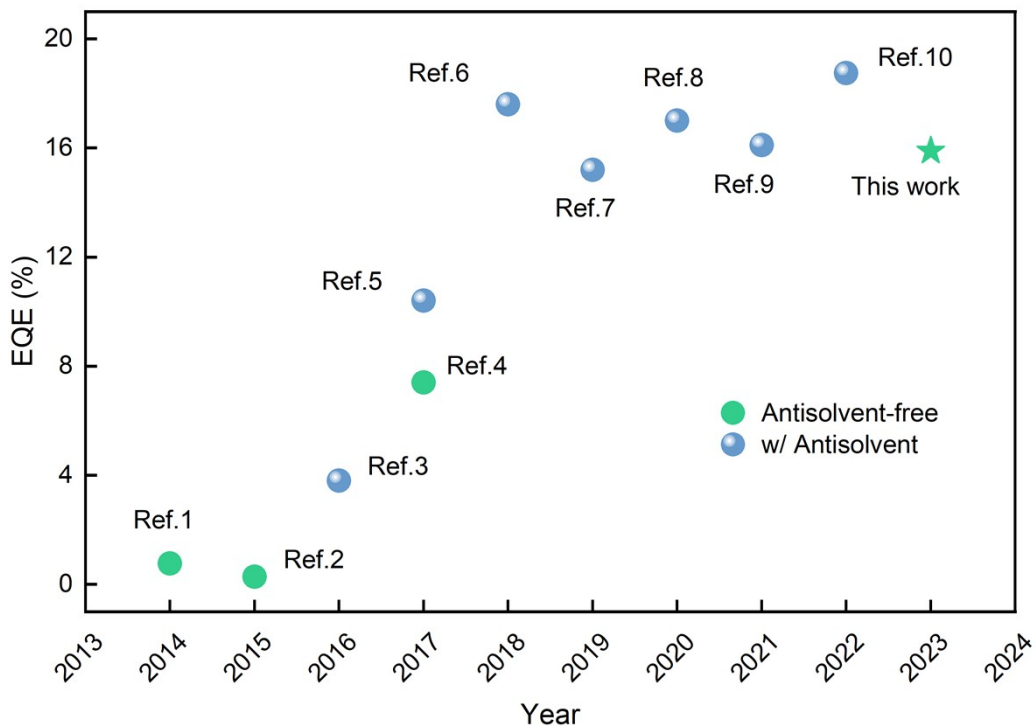


Figure S1. Progress and representative achievements in p-i-n NIR PeLEDs from 2014 to present.^{1–10}

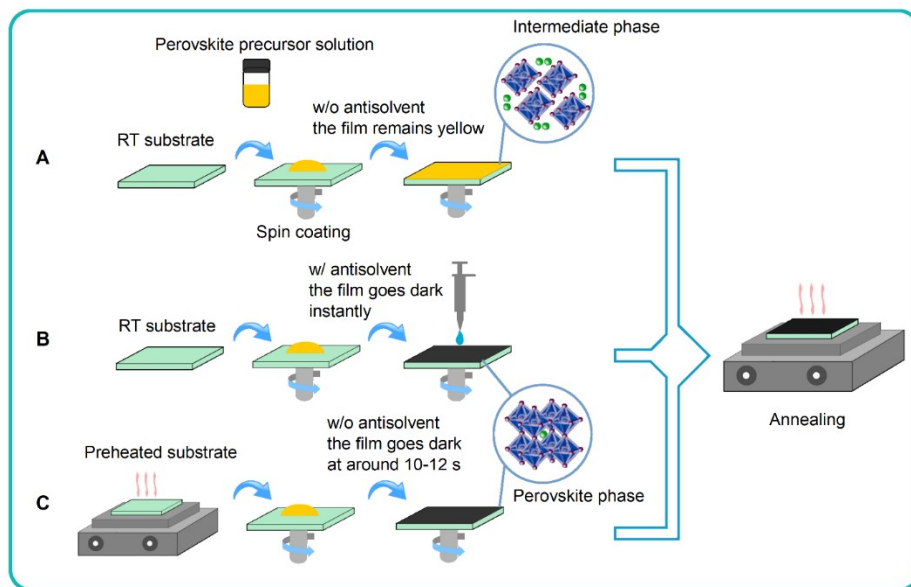


Figure S2. Schematic illustration of deposition process of perovskite emitter layers. (A) Conventional deposition process without antisolvent, (B) Conventional deposition process with antisolvent, and (C) Antisolvent-free with substrate preheating.

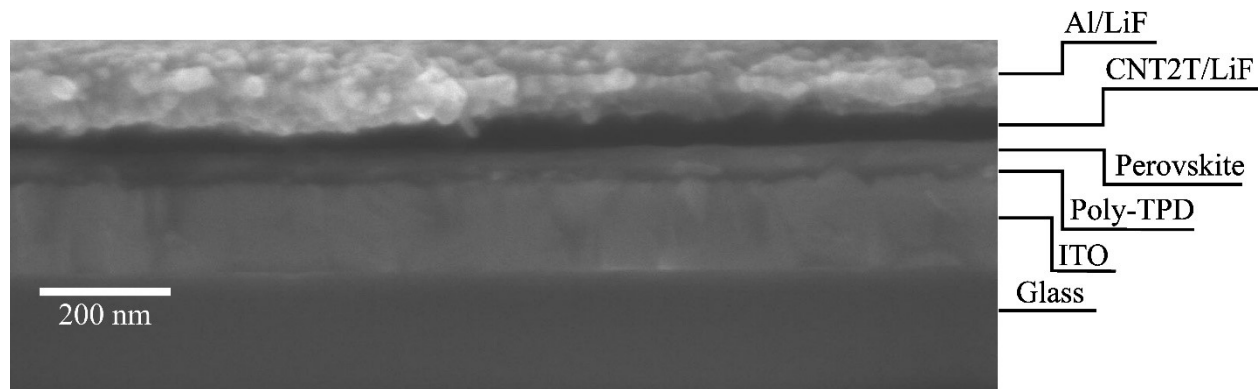


Figure S3. Cross-sectional SEM image of the antisolvent-free NIR PeLEDs.

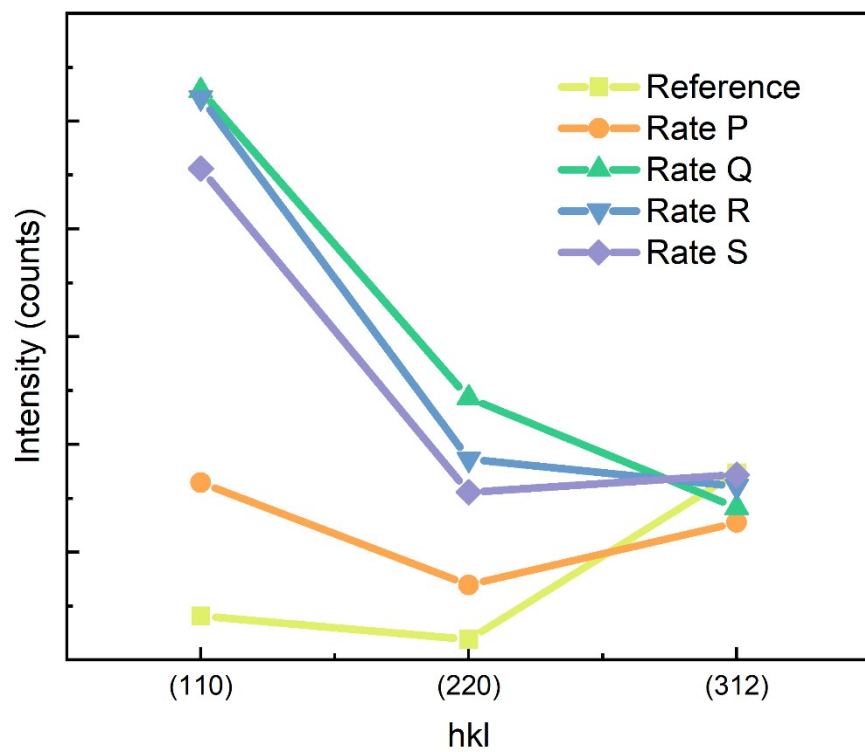


Figure S4. Comparative diffraction intensity at prominent diffraction peaks from XRD pattern.

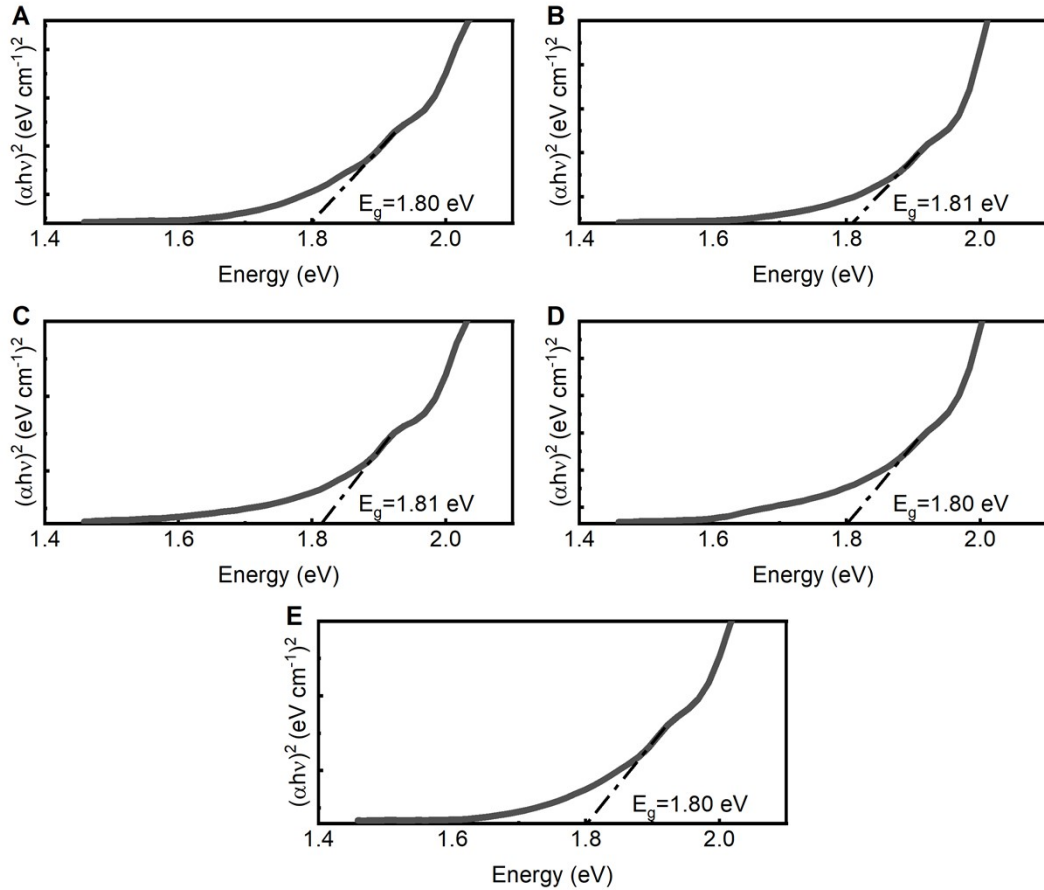


Figure S5. Tauc plot and $(\alpha h\nu)^2$ vs. photon energy ($h\nu$) for the perovskite film with different preheating rate (A) Reference, (B) Rate P, (C) Rate Q, (D) Rate R, and (E) Rate S.

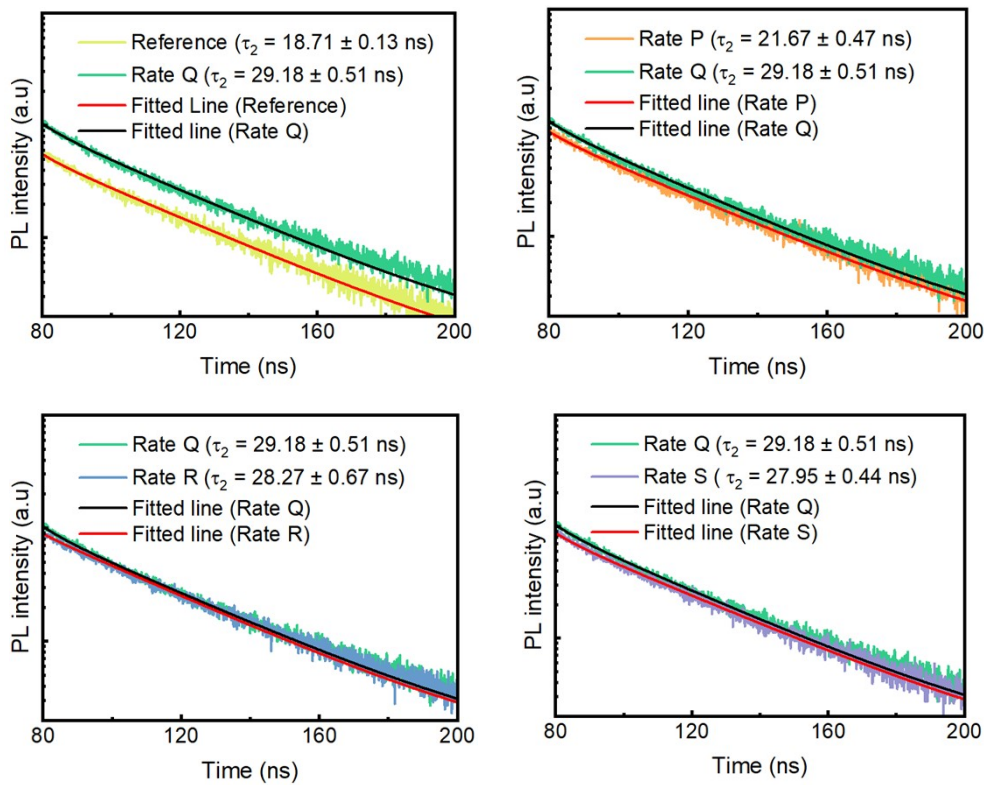


Figure S6. TRPL decay profiles comparison of optimal Rate Q with other samples.

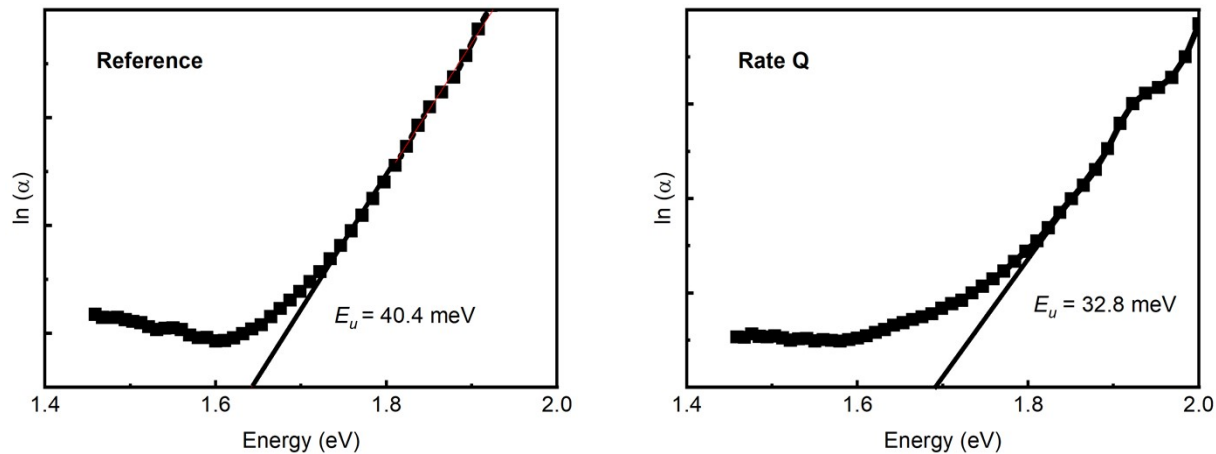


Figure S7. Plot of $\ln(\alpha)$ vs photon energy used to extract the Urbach energy of perovskite films.

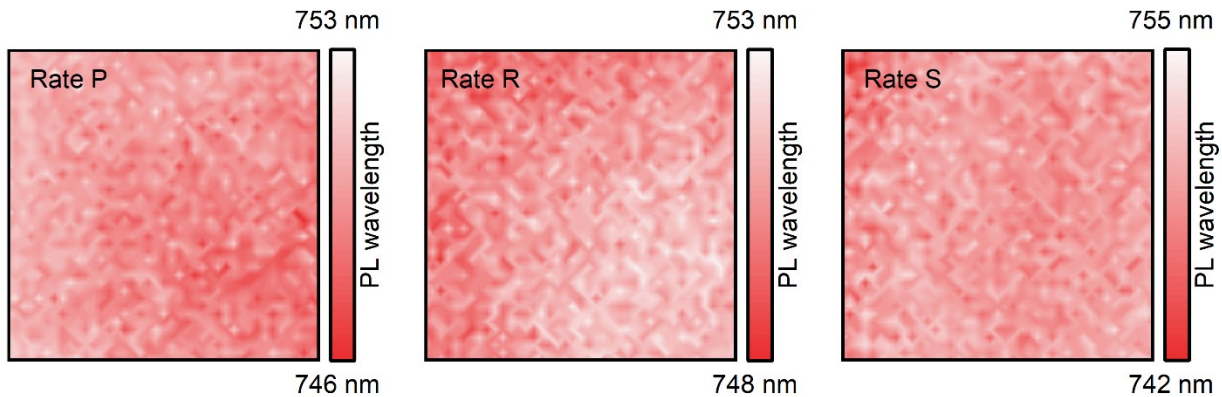


Figure S8. PL mapping of perovskite film with Rate P, R and S.

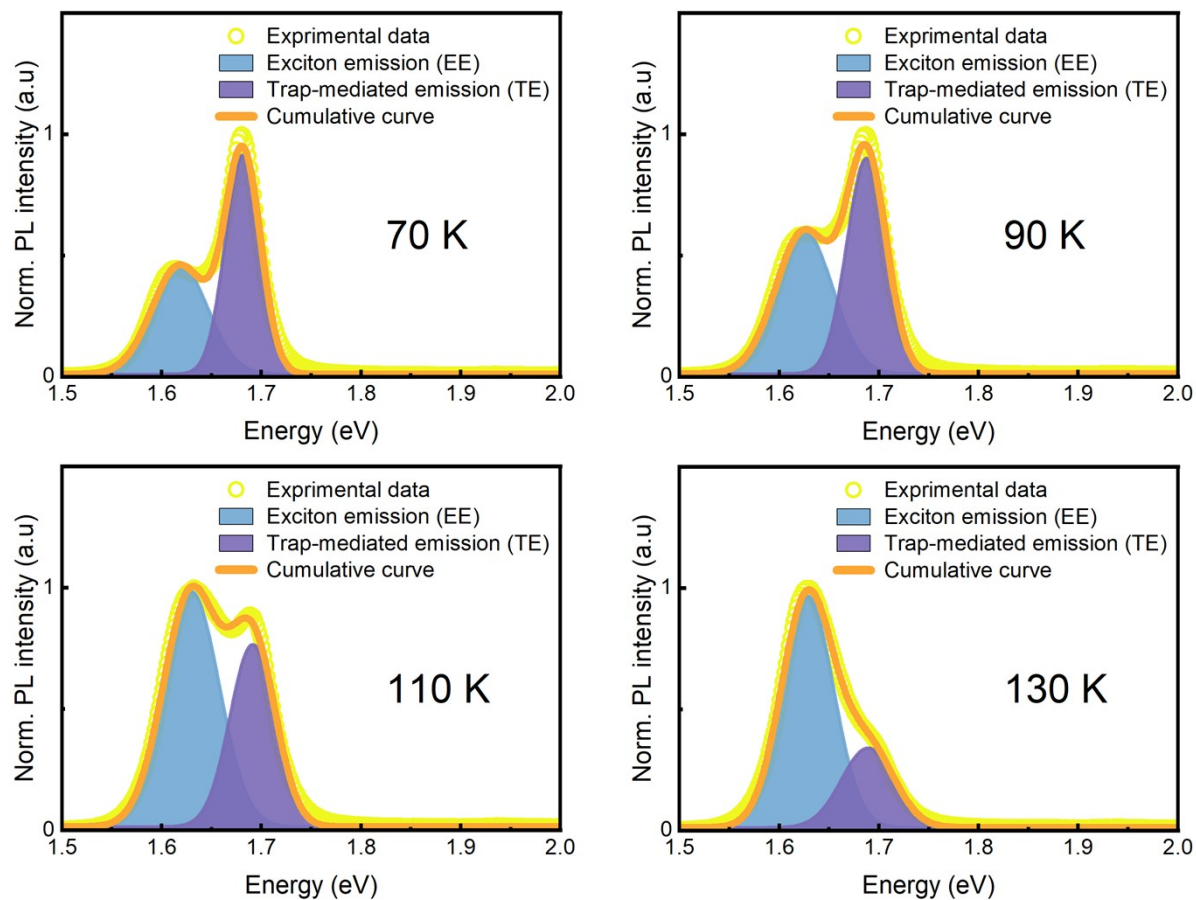


Figure S9. PL emission of Reference perovskite film, according to temperature from 70 K to 130 K. The peaks were deconvoluted into exciton emission and trap-mediated emission.

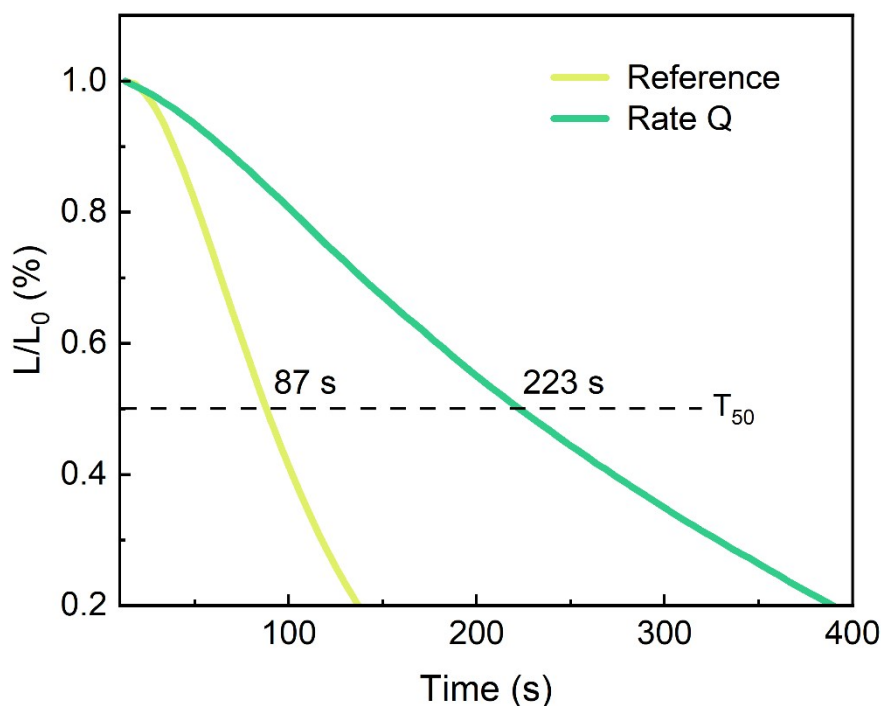


Figure S10. Operating lifetime of the antisolvent-free NIR PeLEDs with encapsulation tested at a constant current density of 5 mA cm^{-2} .

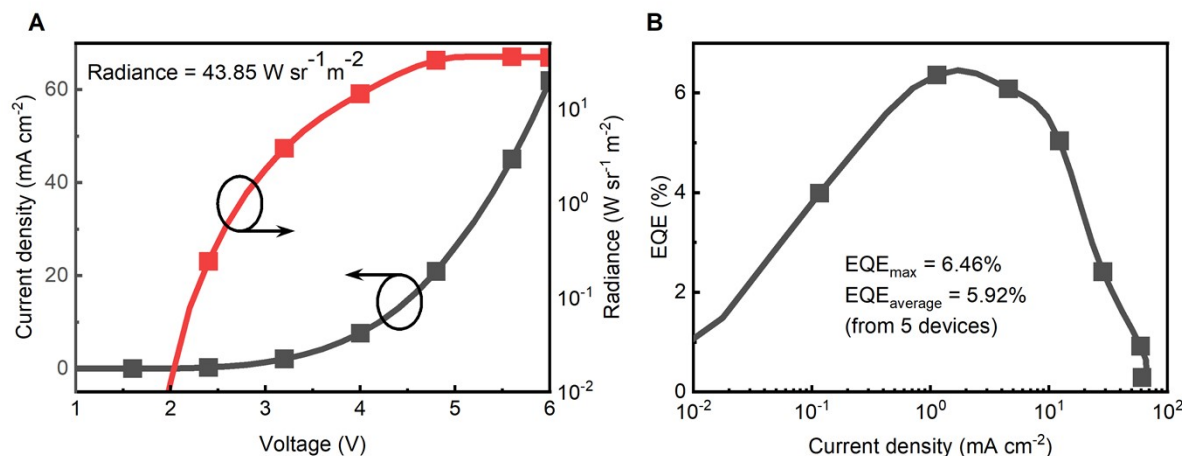


Figure S11. Performance of antisolvent- and annealing-free NIR PeLEDs fabricated with Rate Q (A) J - V - L curves and (B) EQE curves.

The carrier lifetime of the perovskite films is fitted using a bi-exponential decay model as follows (where B_1 and B_2 are the decay amplitudes with lifetimes τ_1 and τ_2 , respectively).¹¹

$$I(t) = B_1 \exp\left(-\frac{t}{\tau_1}\right) + B_2 \exp\left(-\frac{t}{\tau_2}\right)$$

The carrier lifetimes and the decay amplitudes are shown in Table S1.

Table S1. Fitting parameters of time-resolved photoluminescence decay curve.

Sample	$B_{1\pm} err$	$\tau_{1\pm} err$ (ns)	$B_{2\pm} err$	$\tau_{2\pm} err$ (ns)
Reference	23.44 ± 4.84	0.74 ± 0.28	76.56 ± 0.14	18.71 ± 0.13
Rate P	21.08 ± 1.63	1.16 ± 0.83	78.92 ± 0.17	21.67 ± 0.47
Rate Q	9.30 ± 3.97	2.15 ± 0.64	90.7 ± 0.29	29.18 ± 0.51
Rate R	13.78 ± 3.52	1.53 ± 0.49	86.22 ± 0.44	28.27 ± 0.67
Rate S	13.01 ± 1.15	1.77 ± 0.61	86.99 ± 0.62	27.95 ± 0.44

References

- (1) Tan, Z. K.; Moghaddam, R. S.; Lai, M. L.; Docampo, P.; Higler, R.; Deschler, F.; Price, M.; Sadhanala, A.; Pazos, L. M.; Credgington, D.; Hanusch, F.; Bein, T.; Snaith, H. J.; Friend, R. H. Bright Light-Emitting Diodes Based on Organometal Halide Perovskite. *Nat. Nanotechnol.* **2014**, 9 (9), 687–692. <https://doi.org/10.1038/nnano.2014.149>.
- (2) Kumawat, N. K.; Dey, A.; Narasimhan, K. L.; Kabra, D. Near Infrared to Visible Electroluminescent Diodes Based on Organometallic Halide Perovskites: Structural and Optical Investigation. *ACS Photonics* **2015**, 2 (3), 349–354. <https://doi.org/10.1021/acspophotonics.5b00018>.

- (3) Hong, W. L.; Huang, Y. C.; Chang, C. Y.; Zhang, Z. C.; Tsai, H. R.; Chang, N. Y.; Chao, Y. C. Efficient Low-Temperature Solution-Processed Lead-Free Perovskite Infrared Light-Emitting Diodes. *Adv. Mater.* **2016**, *28* (36), 8029–8036. <https://doi.org/10.1002/adma.201601024>.
- (4) Zhao, L.; Gao, J.; Lin, Y. H. L.; Yeh, Y. W.; Lee, K. M.; Yao, N.; Loo, Y. L.; Rand, B. P. Electrical Stress Influences the Efficiency of CH₃NH₃PbI₃ Perovskite Light Emitting Devices. *Adv. Mater.* **2017**, *29* (24), 1–6. <https://doi.org/10.1002/adma.201605317>.
- (5) Xiao, Z.; Kerner, R. A.; Zhao, L.; Tran, N. L.; Lee, K. M.; Koh, T. W.; Scholes, G. D.; Rand, B. P. Efficient Perovskite Light-Emitting Diodes Featuring Nanometre-Sized Crystallites. *Nat. Photonics* **2017**, *11* (2), 108–115. <https://doi.org/10.1038/nphoton.2016.269>.
- (6) Zhao, L.; Lee, K. M.; Roh, K.; Khan, S. U. Z.; Rand, B. P. Improved Outcoupling Efficiency and Stability of Perovskite Light-Emitting Diodes Using Thin Emitting Layers. *Adv. Mater.* **2019**, *31* (2), 1–6. <https://doi.org/10.1002/adma.201805836>.
- (7) Xiao, Z.; Kerner, R. A.; Tran, N.; Zhao, L.; Scholes, G. D.; Rand, B. P. Engineering Perovskite Nanocrystal Surface Termination for Light-Emitting Diodes with External Quantum Efficiency Exceeding 15%. *Adv. Funct. Mater.* **2019**, *29* (11), 1–7. <https://doi.org/10.1002/adfm.201807284>.
- (8) Zhao, L.; Roh, K.; Kacmoli, S.; Al Kurdi, K.; Jhulki, S.; Barlow, S.; Marder, S. R.; Gmachl, C.; Rand, B. P. Thermal Management Enables Bright and Stable Perovskite Light-Emitting Diodes. *Adv. Mater.* **2020**, *32* (25), 1–7. <https://doi.org/10.1002/adma.202000752>.

- (9) Chu, S.; Chen, W.; Fang, Z.; Xiao, X.; Liu, Y.; Chen, J.; Huang, J.; Xiao, Z. Large-Area and Efficient Perovskite Light-Emitting Diodes via Low-Temperature Blade-Coating. *Nat. Commun.* **2021**, *12* (1). <https://doi.org/10.1038/s41467-020-20433-4>.
- (10) Iskandar, J.; Lee, C.; Kurniawan, A.; Iskandar, J.; Lee, C.; Kurniawan, A.; Cheng, H.; Liu, S. Article Improving the Efficiency of Near-IR Perovskite LEDs via Surface Passivation and Ultrathin Interfacial Layers Improving the Efficiency of near-IR Perovskite LEDs via Surface Passivation and Ultrathin Interfacial Layers. *Cell Reports Phys. Sci.* **2022**, *101170*. <https://doi.org/10.1016/j.xcrp.2022.101170>.
- (11) Ghosh, J.; Ghosh, R.; Giri, P. K. Mesoporous Si Nanowire Templatized Controlled Fabrication of Organometal Halide Perovskite Nanoparticles with High Photoluminescence Quantum Yield for Light-Emitting Applications. *ACS Appl. Nano Mater.* **2018**, *1* (4), 1551–1562. <https://doi.org/10.1021/acsanm.8b00047>.